Joint International Topical Meeting on Mathematics & Computation and Supercomputing in Nuclear Applications (M&C + SNA 2007)
Monterey, California, April 15-19, 2007, on CD-ROM, American Nuclear Society, LaGrange Park, IL (2007)

MECHANICAL STRESSES IN FUEL PARTICLES AND GRAPHITE OF HIGH TEMPERATURE REACTORS

B. Boer,[1*] A.M. Ougouag,[2] G.K. Miller,[2] and J.L. Kloosterman[1]
[1]Delft University of Technology
Mekelweg 15, 2629 JB, Delft, the Netherlands
B.Boer@tudelft.nl

[2]Idaho National Laboratory
2525 N. Fremont Av., Idaho Falls, ID, USA

ABSTRACT

TRISO fuel particles in high temperature reactors experience stress due to fission product build up inside the particle, shrinkage/swelling of the Pyrocarbon layers and thermal expansion. In most analyses of stress and strain, the mechanical model consists of a single particle in vacuum. However, in the fuel zone of present day pebble designs, the TRISO particles can be positioned within a relatively short distance from each other and it is therefore likely that the stress field of a given particle influences the stress state of its neighbors. Furthermore, the material in which the particles are embedded experiences dimensional changes under irradiation, which in turn causes additional stress effects on the fuel particles.
In this paper an attempt is made to expand existing visco-elastic models to incorporate the above mentioned effects. It is found that the presence of the matrix material plays a significant role in the determination of the stresses that apply to a single isolated TRISO particle as well as in the transmission of the stresses between particles in actual pebble designs.

Key Words: High Temperature Reactor, fuel particle performance, mechanical stress

1. INTRODUCTION

Present day designs of high temperature reactor fuel for both pebble bed and hexagonal block fuel types consist of coated particles embedded in graphite with varying packing densities. During operation of the reactor these particles experience stresses caused by irradiation.

Gaseous fission products build up inside the particle, which results in a pressure on the Pyrocarbon (PyC) and Silicon carbide (SiC) layers. The Inner (IPyC) and Outer (OPyC) Pyrocarbon layers first shrink and then they subsequently swell during irradiation, while stresses are reduced by irradiation creep. Thermal expansion at increasing reactor operating temperatures during transients can cause additional stress in the particle. Furthermore, the graphite within the particles are embedded undergoes dimensional changes. The stresses in the TRISO particles induced by these combined effects, can be modeled to predict their possible failure for the various proposed fuel designs.

*Corresponding author

In designs with high packing fractions of fuel particles, the stress effects of neighboring fuel particles, on a given particle can also be important and must as well be incorporated in these fuel performance models.

In the following section a stress model is proposed that describes stresses in the different layers of the particle and the surrounding graphite. This model is used to first estimate the stresses within the various layers of a TRISO particle that originate from phenomena within the particle. The model can also be, and is, used to calculate the stress effects of neighboring particles on a given fuel particle.

2. MECHANICAL STRESS IN A TRISO PARTICLE SURROUNDED BY A GRAPHITE LAYER

Analytical methods for modeling stresses in spherical fuel particles were developed in the past. These models consist at most of an Inner Pyrocarbon layer, a Silicon Carbon layer and an Outer Pyrocarbon layer. To account for the stresses in the graphite matrix material in which the TRISO particles are embedded, the 3-layer model of references [1],[2],[3] is expanded with the additional graphite layer (see Fig. 1).

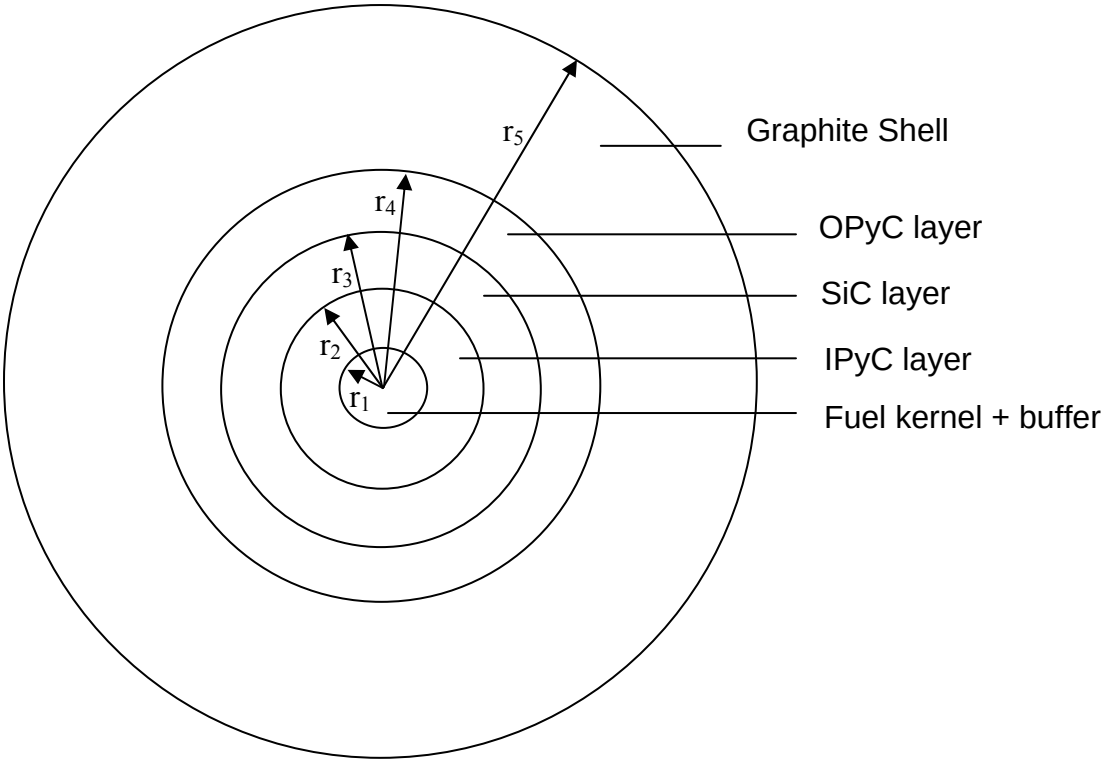

Figure 1. Schematic drawing of a spherical fuel particle in graphite

2.1. Analytical stress model for a spherical fuel particle in graphite

The creep behavior in the pyrocarbon layers of the fuel particle and the graphite matrix can be modeled with a Maxwell creep model. This model assumes that the steady state strain rate is represented by an elastic (spring) and viscous (dashpot) model in series [1].
The strain derivatives for the radial and tangential direction in a spherical element, including irradiation dimensional change source terms and thermal expansion, are given by [1]:

$$\frac{\partial \varepsilon_r}{\partial t} = \frac{1}{E}\left[\frac{\partial \sigma_r}{\partial t} - 2\mu\frac{\partial \sigma_t}{\partial t}\right] + c\left[\left(\sigma_r - 2\nu\sigma_t\right)\right] + \dot{S}_r + \alpha_r\dot{T} \tag{1}$$

$$\frac{\partial \varepsilon_t}{\partial t} = \frac{1}{E}\left[\left(1-\mu\right)\frac{\partial \sigma_t}{\partial t} - \mu\frac{\partial \sigma_r}{\partial t}\right] + c\left[\left(1-\nu\right)\sigma_t - \nu\sigma_r\right] + \dot{S}_t + \alpha_t\dot{T} \tag{2}$$

The first terms on the right-hand side (RHS) of Eqs.(1) and (2) in the brackets represent the elastic behavior of the element. The second term, also within brackets, is the viscous term, which represents creep effects. The last terms in the equations represents swelling or shrinkage of the material under irradiation and thermal expansion.
The strain-displacement relationships and equilibrium equation in a spherical element are as follows:

$$\varepsilon_r = \frac{\partial u}{\partial r} \tag{3}$$

$$\varepsilon_t = \frac{u}{r} \tag{4}$$

$$\sigma_t = \sigma_r + \frac{r}{2}\frac{\partial \sigma_r}{\partial r} \tag{6}$$

The combination of the above equations leads to [1]:

$$r^2\frac{\partial^2 \Delta u}{\partial r^2} + 2r\frac{\partial \Delta u}{\partial r} - 2\Delta u = \frac{2rc\Delta t\left(\mu-\nu\right)}{\left(1-\mu\right)}\left[\frac{r^2}{2}\frac{\partial^2 \sigma_r}{\partial r^2} + 2r\frac{\partial \sigma_r}{\partial r}\right] - \frac{2r\left(1-2\mu\right)\Delta t}{\left(1-\mu\right)}\left(\dot{S}_t + \alpha_t\dot{T} - \dot{S}_r - \alpha_r\dot{T}\right) \tag{7}$$

in which Δu is the incremental change of the radial displacement with dose t.

A general solution for the above equation can be found, which has to be combined with boundary conditions for each layer to find the stress at each position within the sphere. The boundary conditions at each interface imply continuity of radial stress and displacement. The same procedure as in reference [2] is followed for a three layer problem, in which the solution for the radial displacement in integral form is used to implement the boundary conditions. For each layer interface we can equate the displacements:

IPyC outer surface:

$$u_I = a_1 p + a_2 \sigma_{rI} + a_3 \int p c_I dt + a_4 \int \sigma_{rI} c_I dt + a_5 \int \left(\dot{S}_{rI} + \alpha_{rI} \dot{T}_I \right) dt + a_6 \int \left(\dot{S}_{tI} + \alpha_{tI} \dot{T}_I \right) dt \quad (8)$$

SiC inner and outer surface:

$$u_I = b_1 \sigma_{rI} + b_2 \sigma_{rO} + b_3 \int \alpha_{rS} \dot{T}_S dt + b_4 \int \alpha_{tS} \dot{T}_S dt \quad (9)$$

$$u_O = c_1 \sigma_{rI} + c_2 \sigma_{rO} + c_3 \int \alpha_{rS} \dot{T}_S dt + c_4 \int \alpha_{tS} \dot{T}_S dt \quad (10)$$

OPyC inner and outer surface:

$$u_O = d_1 \sigma_{rO} + d_2 \sigma_{rX} + d_3 \int \sigma_{rO} c_O dt + d_4 \int \sigma_{rX} c_O dt + d_5 \int \left(\dot{S}_{rO} + \alpha_{rO} \dot{T}_O \right) dt + d_6 \int \left(\dot{S}_{tO} + \alpha_{tO} \dot{T}_O \right) dt \quad (11)$$

$$u_X = e_1 \sigma_{rO} + e_2 \sigma_{rX} + e_3 \int \sigma_{rO} c_O dt + e_4 \int \sigma_{rX} c_O dt + e_5 \int \left(\dot{S}_{rO} + \alpha_{rO} \dot{T}_O \right) dt + e_6 \int \left(\dot{S}_{tO} + \alpha_{tO} \dot{T}_O \right) dt \quad (12)$$

Graphite-Matrix inner surface:

$$u_X = f_1 \sigma_{rX} + f_2 q + f_3 \int \sigma_{rX} c_X dt + f_4 \int q c_X dt + f_5 \int \left(\dot{S}_{rX} + \alpha_{rX} \dot{T}_X \right) dt + f_6 \int \left(\dot{S}_{tX} + \alpha_{tX} \dot{T}_X \right) dt \quad (13)$$

The coefficients a_i, b_i, c_i, d_i, e_i and f_i are functions of the geometry and the material properties of the layers [2]. The above equations can be combined to find a system of equations for the radial stresses at each layer interface. For the above four-layer problem we obtain a system of three nonhomogeneous linear equations of the form:

$$\dot{\boldsymbol{\sigma}}_r - \boldsymbol{B}\boldsymbol{\sigma}_r = \boldsymbol{g}(t) \quad (14)$$

The solution to this system is [4]:

$$\boldsymbol{\sigma}_r = \mathrm{C}_1 \boldsymbol{\xi}_1 e^{\lambda_1 t} + \mathrm{C}_2 \boldsymbol{\xi}_2 e^{\lambda_2 t} + \mathrm{C}_3 \boldsymbol{\xi}_3 e^{\lambda_3 t} + \boldsymbol{G}_0 + \boldsymbol{G}_1 t \quad (15)$$

where $\boldsymbol{\xi}_i$ and λ_i are the eigenvectors and eigenvalues of the system, respectively, and C_i are constants determined by the initial conditions. The eigenvalues λ_i can be determined as functions of the coefficients B_i. A numerical approach is used to calculate the eigenvalues and eigenvectors.

Once the eigenvalues and vectors are determined, the vectors $\boldsymbol{G_0}$ and $\boldsymbol{G_1}$ can be calculated by means of the method of undetermined coefficients [4]. We can then obtain the radial stresses at each layer interface at each neutron fluence t, with eq.(15). Once these stresses are obtained, the radial and tangential stress within the layers can be easily calculated using the general equations for stress in a spherical layer [2,3],

$$\sigma_r(r,t)=\frac{r_a^3\left(r_b^3-r^3\right)}{r^3\left(r_b^3-r_a^3\right)}p-\frac{r_b^3\left(r_a^3-r^3\right)}{r^3\left(r_b^3-r_a^3\right)}q-\frac{2}{3}\left[\frac{r_a^3\left(r_b^3-r^3\right)\ln r_a-r_b^3\left(r_a^3-r^3\right)\ln r_b}{r^3\left(r_b^3-r_a^3\right)}-\ln r\right]F(t) \quad (16)$$

and

$$\sigma_t(r,t)=-\frac{r_a^3\left(r_b^3+2r^3\right)}{2r^3\left(r_b^3-r_a^3\right)}p+\frac{r_b^3\left(r_a^3+2r^3\right)}{2r^3\left(r_b^3-r_a^3\right)}q+\frac{1}{3}\left[\frac{r_a^3\left(r_b^3+2r^3\right)\ln r_a-r_b^3\left(r_a^3+2r^3\right)\ln r_b}{r^3\left(r_b^3-r_a^3\right)}+2\ln r+1\right]F(t) \quad (17)$$

where r_a and r_b are the inner and outer radius of the layer, respectively, while p and q are the inner and outer pressure on the layer. $F(t)$ is the following function :

$$F(t)=\left[F(t_{n-1})-a_0\right]e^{-\beta(t-t_{n-1})}+a_0 \quad , \quad (18)$$

with,

$$\beta=\frac{cE(1-\nu)}{(1-\mu)} \quad (19)$$

and

$$a_0=\frac{\bar{\dot{S}}_r-\bar{\dot{S}}_t+\bar{\alpha}_r\bar{\dot{T}}-\bar{\alpha}_t\bar{\dot{T}}}{c(1-\nu)} \quad , \quad (20)$$

in which the overline indicates that the relevant property is averaged over the time interval.

2.2. Stress effects by dimensional change of the graphite matrix

TRISO fuel particles are embedded in graphite, which itself experiences irradiation-induced dimensional change and thermal expansion [5]. Quantification of the dimensional change of graphite has been performed during operation of the AVR reactor [5], by measuring the pebble diameter. In Fig. 2, taken from Ref.[5], the dimensional change rate is shown to remain negative throughout the irradiation. Other studies have found that for some graphite material a turn around exists where the dimensional change rate becomes positive [6]. This behavior of graphite matrix shrinking/swelling is incorporated into the stress analysis model by adding a layer of graphite to a three-layer coated particle model. The thickness of this layer is chosen in such a way that its volume is equivalent to the average graphite volume per particle. This thickness assumes that the outer layer of graphite in the pebble is excluded from consideration. For instance, for a pebble containing 15,000 fuel particles and an outer radius of the OPyC of $r_4 = 0.0465$ cm, the layer thickness is 0.058 cm and $r_5 = 0.105$ cm.

The properties of the particle and the graphite that were used for the calculations are shown in Table I. A linear build up of internal pressure was assumed, with a final pressure of 75 MPa. The following relations, depending on neutron fluence t, for the radial and tangential dimensional change rates of the pyrocarbon layers, were adopted [7]:

$$\dot{S}_r=-0.077e^{(-t)}+0.031 \quad (21)$$

$$\dot{S}_t=-0.036e^{(-2.1t)}-0.01 \quad (22)$$

In Fig. 3 it is shown that the presence of the graphite has a significant effect on the tangential stress in the SiC layer. It is noted that the irradiation-induced dimensional change of the fourth layer (graphite) was not taken into account in the calculations High tensile stresses are found in an early stage of the irradiation, for cases in which the graphite has a low irradiation creep constant. A higher value of the creep constant reduces the tangential stress and tends to the solution for a particle without an additional graphite layer. It is noted that the outer surface of the OPyC layer and the graphite matrix remain bonded throughout irradiation.

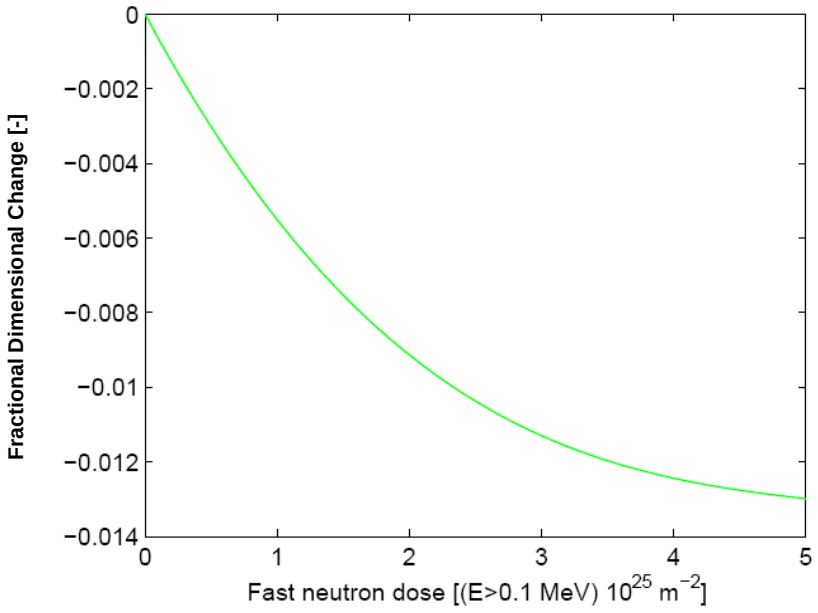

Figure 2. Dimensional change of graphite during operation

Table I. Properties of TRISO particles used in the present stress analysis

Item	Value	Unit
Kernel diameter	500	μm
Buffer layer thickness	95	μm
IPyC layer thickness	40	μm
SiC layer thickness	35	μm
OPyC layer thickness	40	μm
Creep constant of the PyC layers	$3.0\ 10^{-4}$	$(\text{MPa}\ 10^{25}\text{m}^{-2})^{-1}$
PyC Young's modulus	$3.96\ 10^{4}$	MPa
SiC Young's modulus	$4.0\ 10^{5}$	MPa
Graphite Young's modulus	$1.05\ 10^{4}$	MPa
Internal pressure (final)	75	MPa

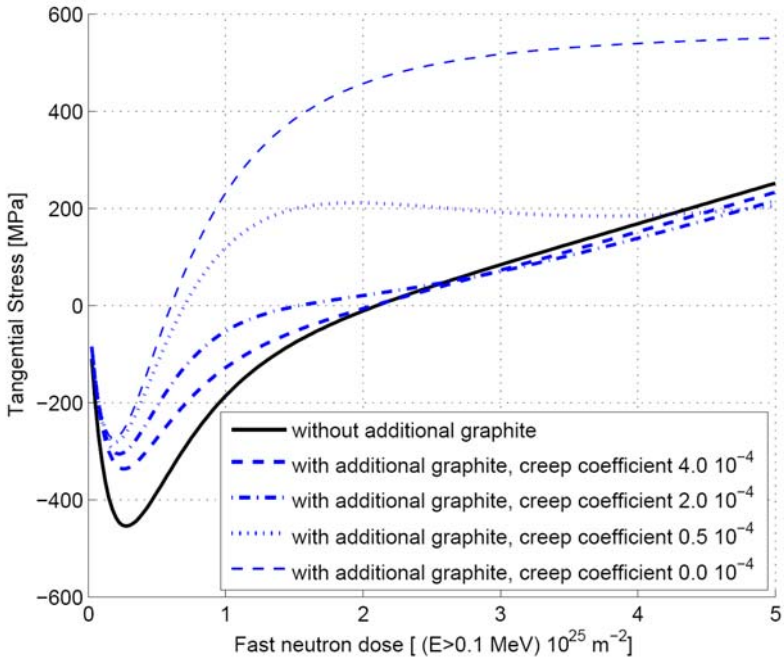

Figure 3. Effect of the presence of graphite on the SiC tangential stress (excluding dimensional change of graphite). The continuous line represents the case without the additional graphite layer, the dashed/dotted lines represent the cases with a graphite layer for several values of the irradiation creep coefficient (c in (MPa. 10^{25} m^{-2})$^{-1}$)

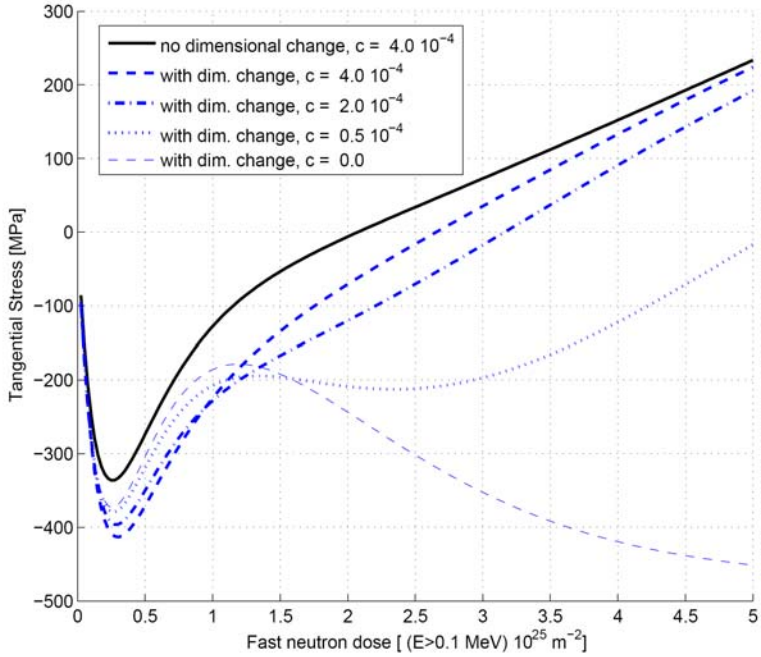

Figure 4. Effect of graphite matrix dimensional change on SiC tangential stress, for several values of the irradiation creep coefficient (c in (MPa. 10^{25} m^{-2})$^{-1}$)

The effect of graphite dimensional change on the SiC tangential stress is shown in Fig. 4, for which the information contained in Fig. 2 was implemented into the stress analysis model. The solid line represents the case in which no dimensional change of the graphite matrix was assumed, while the dashed lines represent cases with dimensional change for various creep constants.

It is concluded that for all cases the dimensional change rate of the graphite layer has a significant impact on the tangential stress of the SiC layer. The dose at which the tangential stress becomes positive depends on the value for the creep coefficient. From references [8, 9] the irradiation creep coefficient for HTGR graphite was determined to be $3.4\ 10^{-29}$-$4.8\ 10^{-29}$ $(\text{MPa m}^{-2})^{-1}$ (for $E > 0.18$ MeV) at 756-984 °C, with an average value of $4.2\ 10^{-29}$ $(\text{MPa m}^{-2})^{-1}$. The latter value is used in the following calculations.

2.3. Stress interaction of a particle with a neighboring fuel particle

A mechanical model is set up to quantify the stresses between two neighboring particles (see Fig. 5). Particles A and B, both with radius R, are at a certain distance *d* from each other. The above presented visco-elastic model is used to calculate the stress field of a given particle that is irradiated, having a zero pressure boundary condition applied at a distance far away from its outer surface. The stress that is present at the particle surface decreases quickly with distance, approximately in proportion with r^{-3} for pure elastic behavior. However, the average inter-particle distance for a pebble with 15,000 particles is just 2 to 3 times the particle radius [10].

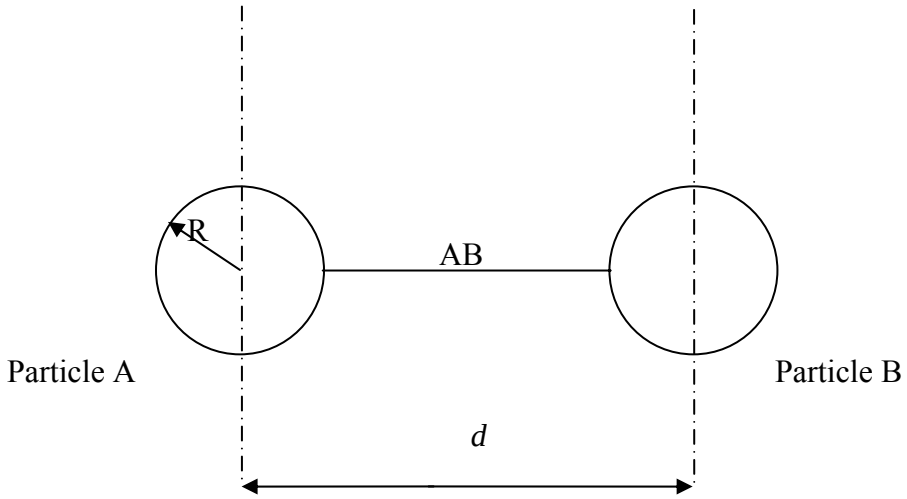

Figure 5: Representation of two neighboring particles

The radial stress fields of the two particles A and B is given in Fig. 6 for a given irradiation time, as well as the combined stress along line AB. Assuming that both particles have the same stress on their surface, the stress along line AB can be calculated by adding the stress fields of the single particles.

In Fig. 6 the solid (magenta) line represents the stress resulting from the presence of particle A. The (green) dashed lines represent the stress resulting from particle B for several positions of particle B with respect to the center of particle A. In Fig. 6, four results of the stress resulting from particle B are shown, corresponding with four possible positions of particle B. The (red) dashed lines represent the sum of the stresses of the two particles for several positions of particle B.

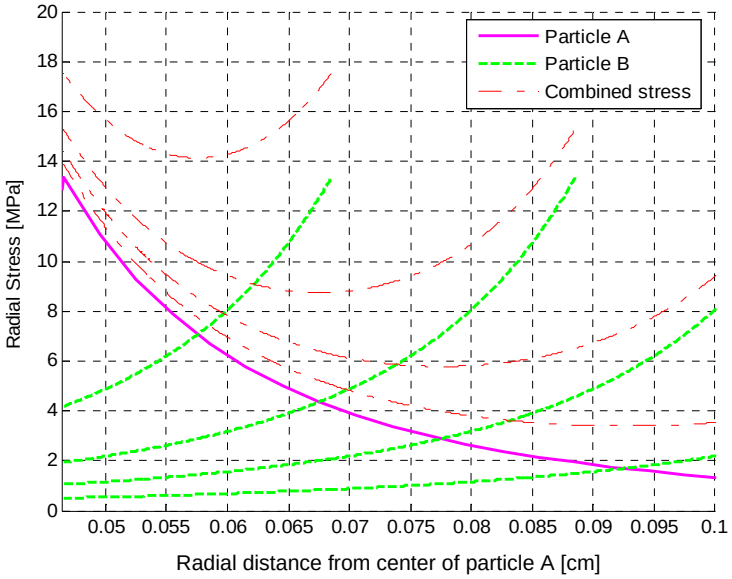

Figure 6. Radial stress fields of two particles and the combined stress field along line AB

One can see that the radial stress at the surface of particle A is not only determined by its own stress, but is also influenced by the presence of its neighbor. If the inter-particle distance is increased, the impact of the neighboring particle decreases (see Fig. 6). However, from reference [10] and as shown in Fig.7, it is known that the inter-particle distance is small. If the inter-particle distance distribution from this reference is used, the average stress increase of a single neighbor at the surface of the particle (along line AB), from the presence of a single neighbor, amounts to a stress increase at the particle surface of about 30 %.

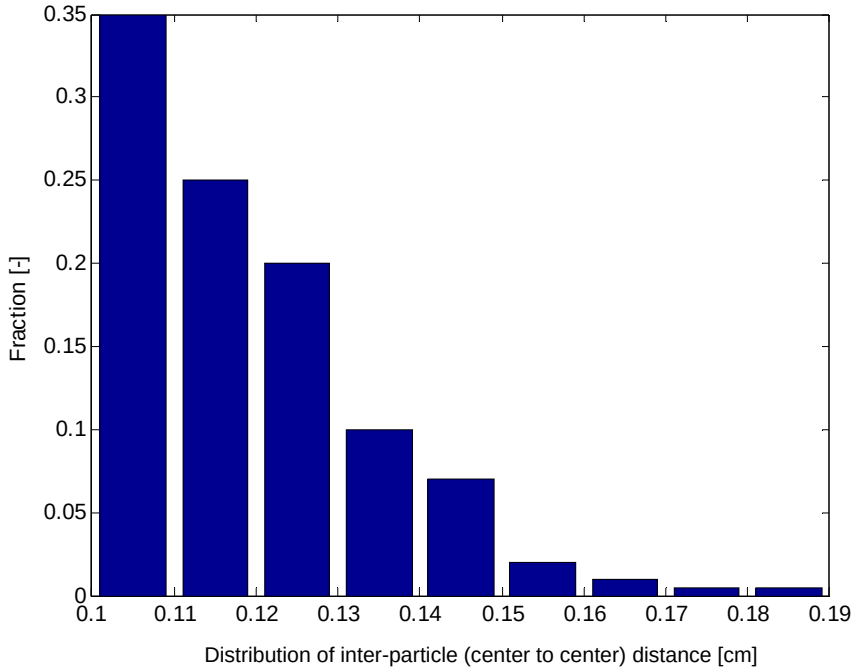

Figure 7. Distribution of inter-particle (center to center) distance in a pebble with 15,000 particles

2.4 Stress interaction of multiple particles

In practical cases a given particle will have several neighboring particles that influence the stress field. The distance of the neighboring particles determines the magnitude of the stress that a given particle sees on its surface.

In practical cases the radial and tangential stress components differ in magnitude and sign (compression or tension). In Fig. 8 the position on a TRISO surface, determined by radius R and angles θ and φ, is denoted with P. At this position on the particle surface, radial and tangential stresses are present, resulting from the particle itself. The radial stress component has the direction of line OP. Furthermore, radial and tangential stresses coming from a neighboring particle, at a distance *d* and with its center at O', are also acting on point P. The direction of the radial stress of the neighboring particle is along line O'P. It must be kept in mind that in practical cases the radius of the particle is in the same order of magnitude as the distance *d*, for the closest neighbors. The magnitude of the radial and tangential stress components can be calculated with Eqs. (17) and (18) respectively, in which *r* is equal to O'P. One can see that the directions of line O'P and OP, which determine the directions of the stresses, do not coincide in general.

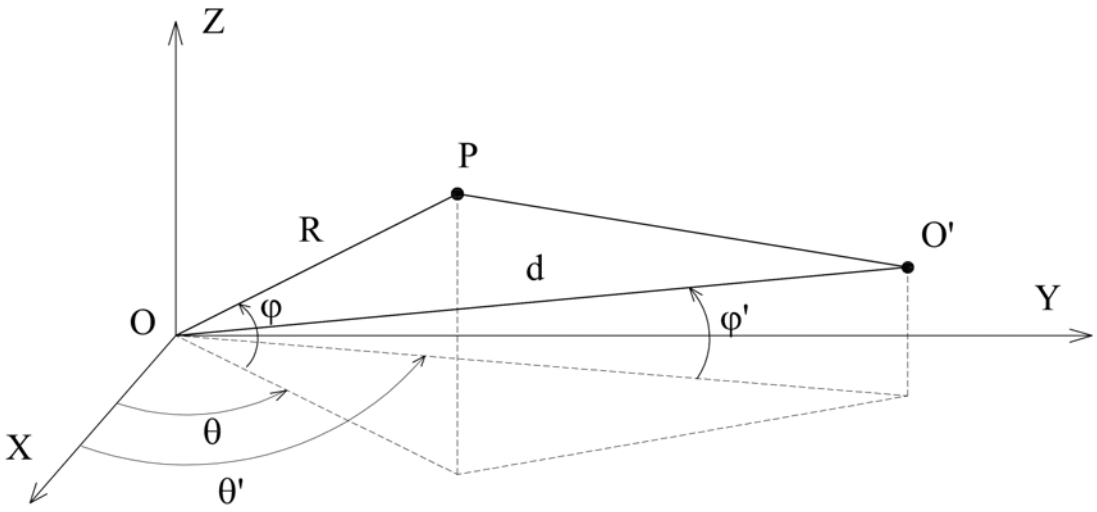

Figure 8. Orientation of a TRISO particle at O and its neighbor at P'

In order to calculate the total stress field, the stress components of the emitting particle are transformed to the stress directions of the receiving particle. This is done by defining a transformation matrix L, consisting of the direction cosines between the two coordinate systems [11]:

$$\boldsymbol{L} = \begin{pmatrix} l_1 & l_2 & l_3 \\ m_1 & m_2 & m_3 \\ n_1 & n_2 & n_3 \end{pmatrix} \tag{23}$$

in which:

$$l_1 = (\boldsymbol{X} \bullet \boldsymbol{X'}) \tag{24}$$

where $\boldsymbol{X}$ and $\boldsymbol{X'}$ are the directions of the X axis of the stress tensor for the particle and its neighbor respectively. The stress components ($\boldsymbol{\sigma'}$) from the neighbor can be transformed to a stress tensor in the coordinate system of the given particle ($\boldsymbol{\sigma}$), with:

$$\boldsymbol{\sigma} = \boldsymbol{L}\boldsymbol{\sigma'}\boldsymbol{L}^T \tag{25}$$

This procedure is applied to several neighboring particles, assuming that all neighbors have the same stress state and that the stresses can be superimposed. Because of the nonlinear behavior of the creep, the actual combined stress from multi-particle effects should result in slightly more creep strain (and consequently more stress relief in the graphite) than will be calculated from summing individual particle results.

From Eqs. (17) and (18) it is seen that the magnitude of the stresses decrease as $1/r^3$. However, the number of neighboring particles at a given distance increases proportionally to r^2. Therefore,

the presence of the neighbors, which are within considerable distance from the particle under consideration, results in a small stress contribution per neighbor. However, the total contribution of all particles at this distance can still be significant.

For the sake of model development, it is first considered that the particles are distributed regularly in the matrix material. Fig. 9 shows a cubic distribution of particles. A hexagonal and a random distribution are also considered in this paper. The combined maximum principal stress resulting from all neighbors within a certain distance is presented in Fig. 10 for a cubic distribution of the neighbors.

The inter-particle stress effect is determined, by calculating the principal stresses for several points on the surface of the particle. In Fig. 10 the maximum principal stress is presented, as a function of the distance from the particle. With increasing distance, the number of neighbors to be taken into account increases, assuming that the particle considered is in the middle of the pebble. At a large distance the stress effect from the neighbors becomes small. However, this distance is considerable with regard to the particle diameter. On the other hand, a large part of the effect is determined by the closest neighbors. This can also be concluded from the stress effect for randomly distributed neighbors. The standard deviation from the average stress effect is also presented in Fig. 10 and shows a large spread, especially for short distances. In the random distribution a neighbor can be a short distance from the particle, which results in a large effect on the stress. This can explain the somewhat higher effect for the random distribution, which results in an increase of 40% in the radial stress at the surface of the particle, over the stresses in regular lattices.

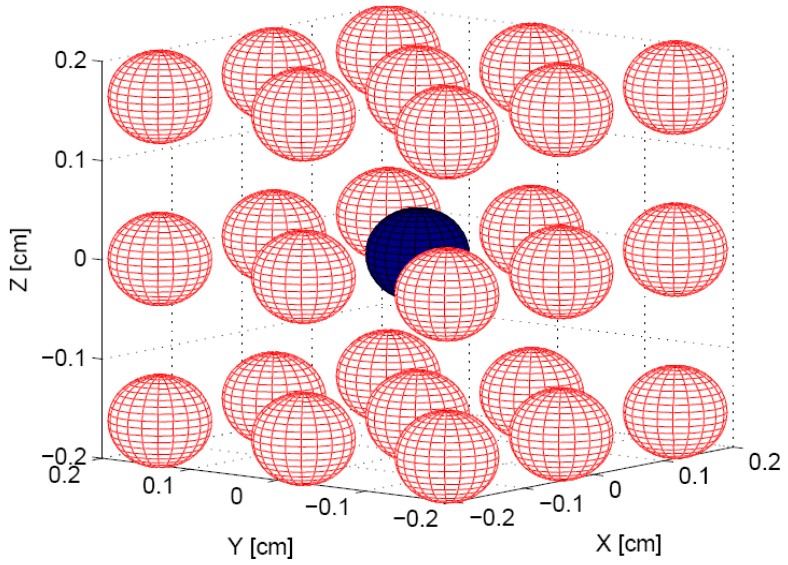

Figure 9. Position of neighboring particles (light/red) with regard to a given particle (dark/blue) for a cubic lattice

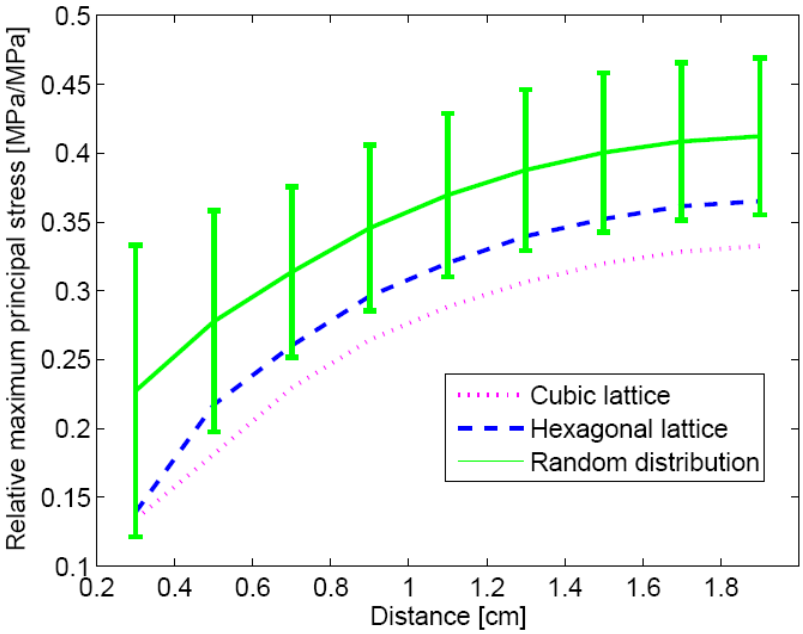

Figure 10. Maximum principal stress normalized to a radial stress of 1 MPa at the surface of the TRISO particles, resulting from neighbors within the specified distance from the particle

The above calculations were performed for a pebble containing 15,000 TRISO particles. Fig. 11 shows the dependency of the relative maximum principal stress on the number of particles contained in the pebble (for a cubic distribution, by considering neighbors within a distance of 0.3 cm). One can see that the stress effect has a quasi-linear dependency on the particle packing fraction.

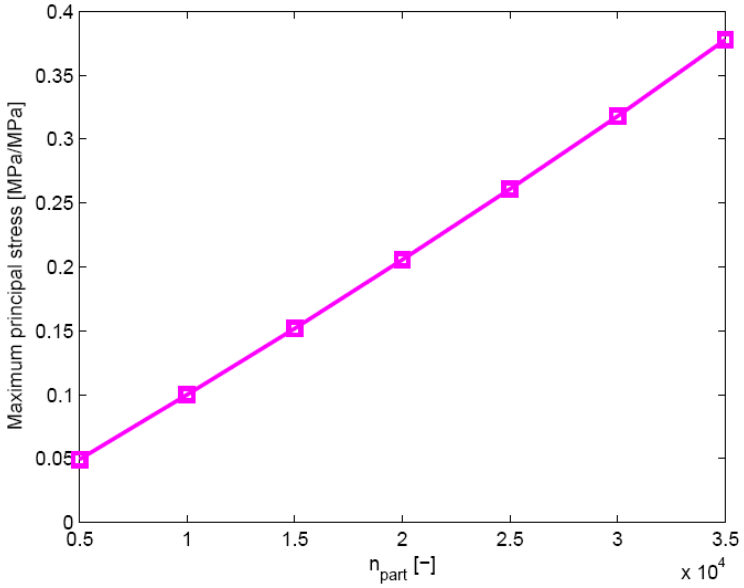

Figure 11: Maximum principal stress dependent on the number of particles in a pebble

In the above analysis it was found that the inter-particle stress effect was in the order of 40 % of the radial stress at the outer surface of a particle for a pebble containing 15,000 TRISO particles that are randomly distributed. Fig. 12 shows the radial stress at the surface of a particle during irradiation, calculated with the 4-layer model and assuming the same conditions as in section 3.2 (excluding the effect of the graphite matrix dimensional change).

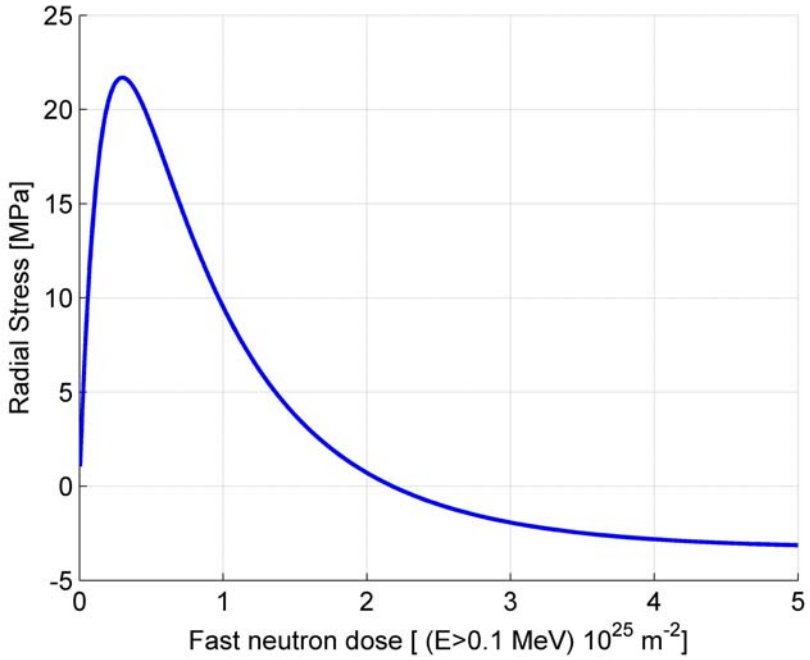

Figure 12. Radial stress at the outer surface of the OPyC of a TRISO particle during irradiation

To quantify the inter-particle effect, the radial stress presented in Fig.12 is used in a 3-layer model as boundary condition to calculate the effect on the tangential stress in the SiC layer. The radial stress on the surface is therefore increased by a factor between 1 and 2. The results are shown in Fig.13. One can recognize a small effect on the SiC tangential stress for the case of 40 % stress increase (factor 1.4), especially at the beginning of the irradiation. In general the tangential stress is reduced for this irradiation case, being either less compressive or less tensile.

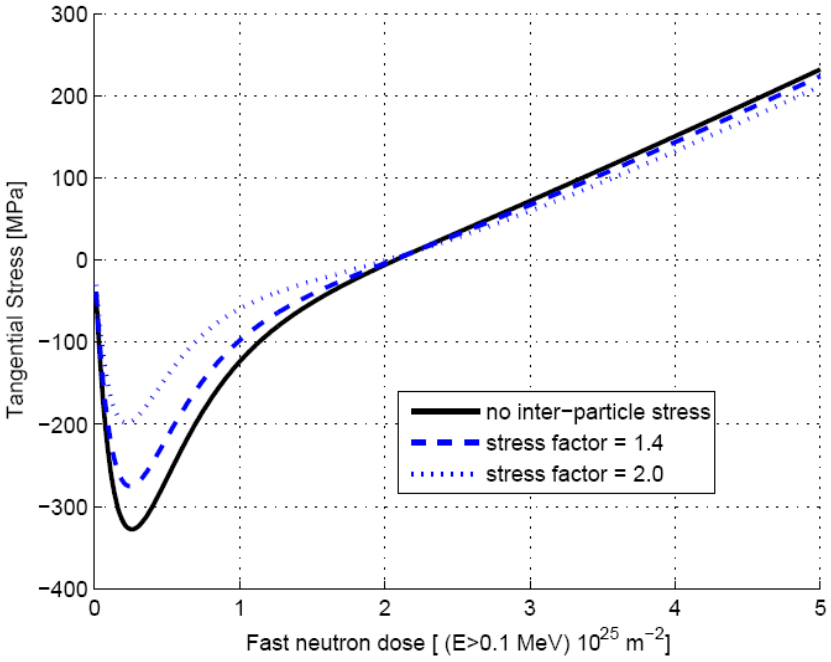

Figure 13. Tangential stress of the SiC layer for several values of radial stress increase on the outer surface of the particle, which represents the inter-particle stress effect

3. CONCLUSIONS

A mechanical model was set up to analyze the stresses in coated particle fuel and the surrounding graphite. It is found that the dimensional change of the graphite has a significant effect on the stresses in the fuel particles.

Furthermore, the stress situation of a neighboring fuel particle can influence the stresses in a given particle. It is found that the closest neighboring particle increases the radial stress at the surface of the particle by 30 % on average for a pebble containing 15,000 particles. Taking into account all neighboring particles in a pebble, an increase of 40 % was found, assuming that the particles are randomly distributed in the fuel zone of the pebble and that the stresses of each individual neighboring particle can be superimposed. It is shown that the effect of the inter-particle stress on the tangential stress in the SiC is small but significant at low neutron fluence. A better treatment of the nonlinearity of the creep in the superposition of the multi-particle stresses is considered to be part of future work.

ACKNOWLEDGMENTS

This paper was written after an internship of B. Boer at the Idaho National Laboratory (INL) in the summer of 2006. The first author would like to thank Drs. A.M. Ougouag, G.K. Miller and other colleagues at the INL for their support during this internship. This work was supported in part by the Next Generation Nuclear Plant (NGNP) project at the INL, under the auspices of the Department of Energy, Office of Nuclear Energy, Science and Technology, under DOE Idaho Operations Office Contract DE-AC07-99ID13727.

REFERENCES

1. G.K. Miller and R.G. Bennett, "Analytical solutions for stresses and displacements in TRISO-coated particles,"*Journal of Nuclear Materials*, **206**, 35-49 (1993)
2. G.K. Miller et al., "Updated solutions for stresses and displacements in TRISO-coated fuel particles," *Engineering Design File (internal INL document)*, **7042** (2006),
3. G.K. Miller, "Stresses in a spherical pressure vessel undergoing creep and dimensional changes," *Int. J. Solids Structures,* **32**, no.14, 2077-2093 (1995)
4. W.E. Boyce and R.C. DiPrima, "Elementary differential equations and boundary value problems," *John Wiley & Sons, Inc. ISBN 0-471-08955-9,* (1992)
5. R. Gontard and H. Nabielek, " Performance Evaluation of Modern HTR TRISO fuels", *HTA-IB-05/90*, Forschz. Juelich, Germany
6. B.J. Marsden, "Irradiation damage in graphite," IAEA-TECDOC-901 XA9642900, International Atomic Energy Agency, 17-46 (1995).
7. D. Petti et al., "Development of Improved Models and Designs for Coated-Particle Fuels," *INEEL/EXT-0200369*, Idaho National Engineering and Environmental Laboratory, (2002)
8. T. Oku, M. Eto, and S. Ishiyama,"Irradiation properties and strength of a fine-grained isotropic graphite,"*Journal of Nuclear Materials*, **172,**77-84, (1990)
9. T. Oku and M. Ishihara, "Lifetime evaluation of graphite components for HTGRs ", *Nuclear Engineering and Design,* **227**,209-217, (2004).
10. A.M. Ougouag, J.L. Kloosterman, W.F.G. van Rooijen, H.D. Gougar and W.K. Terry, " Investigation of Bounds on Particle Packing in Pebble-Bed High Temperature Reactors," *Nuclear Engineering and Design,* **236**, 669-676 (2006).
11. W.B. Bickford,"Advanced mechanics of materials," *Addison Wesley Longman, Inc.*, *ISBN 0-673-98195-9,* (1998)